TIEG1-NULL OSTEOCYTES DISPLAY DEFECTS IN THEIR MORPHOLOGY, DENSITY AND SURROUNDING BONE MATRIX

Oualid Haddad, John R Hawse, Malayannan Subramaniam, Thomas C Spelsberg, Sabine F Bensamoun

Published in final edited form as:
J Musculoskelet Res. 2009 September ; 12(3): 127–136. doi:10.1142/S0218957709002304.

TIEG1-NULL OSTEOCYTES DISPLAY DEFECTS IN THEIR MORPHOLOGY, DENSITY AND SURROUNDING BONE MATRIX

Oualid Haddad[*,‡], **John R. Hawse**[†], **Malayannan Subramaniam**[†], **Thomas C. Spelsberg**[†], and **Sabine F. Bensamoun**[*]

[*]Laboratoire de Biomécanique et Bioingénierie UMR CNRS 6600 Université de Technologie de Compiègne, Compiègne, France

[†]Department of Biochemistry and Molecular Biology Mayo Clinic College of Medicine, Rochester, Minnesota, USA

Abstract

Through the development of TGFβ-inducible early gene-1 (TIEG1) knockout (KO) mice, we have demonstrated that TIEG1 plays an important role in osteoblast-mediated bone mineralization, and in bone resistance to mechanical strain. To further investigate the influence of TIEG1 in skeletal maintenance, osteocytes were analyzed by transmission electron microscopy using TIEG1 KO and wild-type mouse femurs at one, three and eight months of age. The results revealed an age-dependent change in osteocyte surface and density, suggesting a role for TIEG1 in osteocyte development. Moreover, there was a decrease in the amount of hypomineralized bone matrix surrounding the osteocytes in TIEG1 KO mice relative to wild-type controls. While little is known about the function or importance of this hypomineralized bone matrix immediately adjacent to osteocytes, this study reveals significant differences in this bone microenvironment and suggests that osteocyte function may be compromised in the absence of TIEG1 expression.

Keywords

Osteocyte; Bone remodeling; Cell morphology; Transmission Electron Microscopy

INTRODUCTION

Osteocytes are the most abundant cells found in bone tissue. They are networked to each other and to cells on the bone surface via long cytoplasmic extensions through canaliculi. They constitute a three-dimensional (3D) network which seems to be necessary in cell–cell communication, mechanosensing and in osteoblasts and osteoclasts regulation, which are implicated in bone formation and resorption, respectively.[5,21] Moreover, studies have also shown that osteocytes are known to play a role in bone mineral metabolism[9] and the maintenance of their surrounding bone matrix.[19]

Many studies have confirmed the hypothesis that osteocytes are mechanosensors, producing a signal in response to mechanical loading, by sensing stress on bone surfaces through stretch-activated ion channels,[8] flow of interstitial fluid[7,18,35] and electrical potentials.[12] Thus, it is very likely that osteocytes sense mechanical changes and initiate bone

Correspondence to: Dr. Oualid Haddad, PhD, Université de Technologie de Compiègne (UTC), Laboratoire de Biomécanique et Bioingenierie – UMR CNRS 6600, BP 20529, 60205 Compiègne Cedex, France.
[‡]oualid.haddad@utc.fr

remodeling[20] but the precise mechanisms by which this phenomenon occurs are still unclear.

The morphological properties of osteocytes were characterized with different microscopic techniques such as confocal microscopy and Transmission Electron Microscopy (TEM). Using confocal microscopy, Vatsa *et al.*[33] showed that osteocyte lacunae in the fibula are aligned parallel to the mechanical loading direction, whereas those of the calvaria are not aligned in any particular direction, suggesting that osteocytes are able to adapt their morphological properties (anisotropy, shape) to the applied stress. In addition, Irie *et al.*[14] demonstrated that osteocyte maturation is triggered by the mineralization of the surrounding matrix and also observed an increase in osteocytes size when the mineralization around the cells is inhibited by BiPhos-phonate. Additionally, McCreadie *et al.*[22] have shown that the size and shape of osteocytes do not play a role in osteoporotic fractures while Rubin and Jasiuk[24] have demonstrated alterations in lamellar structures for osteoporotic trabecular bone. Moreover, osteocyte density and lacunar density decrease with age in both men and women.[32]

Numerous studies have demonstrated that TGFβ is involved in osteogenesis and plays critical roles in the regulation of bone growth, cell proliferation and differentiation of osteoblasts.[11,16] The absence of TGFβ receptors in osteoblast cells *in vivo* results in decreased osteocyte density and bone turnover.[10] TGFβ-inducible early gene-1 (TIEG1) is a transcription factor which is rapidly induced in osteoblasts following TGFβ stimulation.[25] TIEG1 belongs to the Krüppel-like family of transcription factors including TIEG2 and TIEG3[29,34] and is known to regulate gene expression through the modulation of Smad 2 and Smad 7. This modulation ultimately enhances the TGFβ signal transduction pathway.[15] TIEG1 knockout (KO) mice display a number of bone defects including decreased osteocyte density as well as defects in bone strength and microarchitecture.[3] Osteoblasts isolated from TIEG1 KO mice also display decreased expression of important osteoblast marker genes and exhibit decreased rates of mineralization.[27] Additional studies have revealed microarchitecture changes in both cortical and trabecular bone in TIEG1 KO mice which is correlated with decreased bone strength and osteocytes density.[3,13] The purpose of the present study is to further elucidate the role of TIEG1 in osteocyte development as well as to characterize the morphological properties of osteocytes present in TIEG1 KO mouse bones.

MATERIALS AND METHODS

Animals

TIEG1$^{-/-}$ mice were developed in a C57BL/6 background as described previously.[27] Mice were housed in a temperature-controlled room (22 ± 2°C) with a light/dark cycle of 12 hours. All mice had free access to water and were fed standard laboratory chow (Laboratory Rodent Diet 5001; PMI Feeds, Richmond, VA) *ad libitum*. To reduce variability among experiments, WT and TIEG$^{-/-}$littermates were utilized in all of the experiments performed in these studies. The Institutional Animal Care and Use Committee (IACUC) approved all animal care and experimental procedures.

Bone Section Preparation

A total of 20 C57BL/6 female mice, 10 wild-type (TIEG1$^{+/+}$) and 10 knockout (TIEG1$^{-/-}$) mice were utilized in this study. Mice were analyzed at three different ages to represent young animals (1 month old: M1), adult animals (3 months old: M3) and aged animals (8 months old: M8). A total of three WT and KO mice were sacrificed at 1 month, four WT and KO animals at 3 months and three WT and KO animals at the 8-month time point. After sacrificing, mice were stored at −80°C until use. The left femurs of all mice were removed

and all of the surrounding soft tissue was dissected away. The femurs were then sectioned transversely in the middle of the shaft (1-mm thickness) with a low-speed diamond saw (MT Micro, BROT Technologies, France) under wet conditions.

Bone Sample Processing for Transmission Electron Microscopy

Cross-sections were immediately placed into freshly prepared fixative solution [2% glutaraldehyde, 4% paraformaldehyde in 0.05-M cacodylate buffer at pH 7.4, with 0.7% ruthenium hexammine trichloride (RHT)]. Fixation and decalcification were enhanced using a PELCO BioWave 34700 laboratory microwave (Ted Pella, Inc., Redding, CA). For fixation, samples were kept in the fixative for a minimum of 24 hours and microwaved prior to processing, one minute on, one minute off, one minute on, using a power level of 1 (105 W). After brief washes in 0.1-M phosphate buffer, samples were decalcified by placing into 10% EDTA containing 0.7% RHT and microwaved at power level 6 (700 W) for three hours. A load cooler was used in the microwave to recirculate about one liter of water to cool the EDTA (Ethylene Diamine Tetraacetic Acid) solution during the decalcification process. Following another brief wash in 0.1-M phosphate buffer, samples were microwaved in 1% OsO_4 for one minute on, one minute off, one minute on, 30 minutes off, using a power level of 1 (105 W).

Dehydration of all samples was performed in the microwave using a series of ethanol solutions (60%, 70%, 80%, 95%, 100%, 100%). Samples were microwaved for 40 seconds using a power level of 1 (105 W) during each dehydration step. Infiltration involved 1:1 and 2:1 mixtures of Embed 812/araldite:ethanol in the microwave for five minutes using a power level of 3 (227 W), followed by five minutes at a power level of 4 (385 W) in 100% resin.

Samples were placed into fresh resin overnight and then polymerized in a 65°C oven. Ultrathin (0.1 μm) sections were stained with 2% uranyl acetate and lead citrate. All micrographs were acquired using a transmission electron microscope (Technai G^2 12) equipped with an AMT (Advanced Microscopy Techniques Corp., Danvers, MA) CCD camera.

Image Analysis

For each bone section, 20 images of endosteal osteocytes at high magnification (×11, 000) (Fig. 1) and 10 images of osteocytes at low magnification (×1000) were analyzed, representing a total of 600 images for the 10 WT and 10 KO mice. Morphological parameters characterizing endosteal osteocytes and their surrounding hypomineralized bone matrix were determined as a function of age, using ImageJ software (NIH Image, Bethesda, USA). Using high magnification, the edges of the osteocytes were outlined manually on TEM images allowing for the determination of the cell surfaces (S). To distinguish mineralized area from hypomineralized area, a threshold was performed on TEM images in order to identify the hypomineralized perilacunar matrix (Fig. 2). Then the boundaries of the hypomineralized surfaces (HS) were outlined manually and the HS was calculated. In addition, only the surfaces (S) higher than 10 μm^2 were selected in order to have a representative surface of the cell. The HS was calculated as the difference between the surface outlined with the dotted line representing the edge of the hypomineralized bone matrix surrounding each osteocyte and the osteocyte surface (Fig. 1). To determine osteocyte density, low-magnification (×1000) images were taken of the femoral cross-sections. Osteocytes were counted across the entire surface of each cross-section and osteocyte density was calculated as the number of osteocytes per 100 μm^2 of total bone.

Statistical Analysis

Unpaired *t*-tests were performed using software R (Lucent Technologies, USA) to compare the morphological parameters [cell surface (S), hypomineralized surface (HS)] and osteocyte density between the three experimental groups composed of WT and TIEG1 KO mice.

RESULTS

Effect of Age on Osteocyte Surface

The effect of age on osteocyte surface was determined for both WT and TIEG1 KO mice and is depicted in Fig. 3. The average osteocyte surface (*S*) for WT animals was unchanged between one and three months of age ($S_{M1+/+} = 18.7 \pm 4.9\mu m^2$ versus $S_{M3+/+} = 20.0 \pm 6.2\mu m^2$), but was significantly decreased (20%) by eight months of age ($S_{M8+/+} = 16.4 \pm 5.2\mu m^2$).

However, the average osteocyte surface for TIEG1 KO animals was significantly decreased between one and three months of age ($S_{M1-/-} = 19.5 \pm 6.1\mu m^2$ and $S_{M3-/-} = 16.9 \pm 5.3\mu m^2$) but remained stable at eight month time point ($S_{M8-/-} = 16.2 \pm 4.3\ \mu m^2$). These data reveal that TIEG1 KO osteocyte surface decreases at an early age relative to WT controls. When the data were analyzed with respect to genotype, it was determined that there was no significant difference between the osteocyte surface of WT and TIEG1 KO mice at the one and eight month time points. However, at the three month time point, the osteocyte surface was significantly higher in WT mice relative to TIEG1 KO mice ($S_{M3+/+} = 20.0 \pm 6.2\ \mu m^2$ versus $S_{M3-/-} = 16.9 \pm 5.3\ \mu m^2$).

Effect of Genotype on Hypomineralized Bone Matrix Surrounding Osteocytes

TEM acquisitions of femoral cross-sections reveal that WT osteocytes have a larger area of hypomineralized bone matrix immediately surrounding each osteocyte relative to TIEG1 KO osteocytes (Fig. 1). The average hypomineralized surface (*HS*) surrounding WT osteocytes was unchanged between one and three months of age ($HS_{M1+/+} = 18.3 \pm 6.9\mu m^2$ versus $HS_{M3+/+} = 19.4 \pm 7.2\mu m^2$), while a 25% decrease was observed by eight months of age ($HS_{M8+/+} = 14.2 \pm 5.5\mu m^2$) (Fig. 4). For TIEG1 KO mice, the average *HS* was similar at one, three and eight months of age ($HS_{M1-/-} = 8.0 \pm 4.0\mu m^2$, $HS_{M3-/-} = 8.2 \pm 4.2\mu m^2$ and $HS_{M8-/-} = 8.4 \pm 4.4\mu m^2$) (Fig. 4). When the hypomineralized bone matrix area was compared between WT and TIEG1 KO animals, a highly significant reduction of approximately two-fold was observed within each age group.

Effect of Genotype on Osteocyte Density

Osteocyte density was determined at one, three and eight months of age for WT and TIEG1 KO mice using low-magnification (×1000) transmission electron microscopy [Fig. 5(a)]. These data revealed a significant decrease in femoral osteocyte density between TIEG1 KO and WT mice for each age group analyzed. Specifically, there was a 15% decrease at one month of age, a 41% decrease at three months of age and 22% decrease at eight months of age [Fig. 5(b)].

Interestingly, osteocyte density in both WT and TIEG1 KO mice displayed significant differences with age. Between one and three months of age, the WT osteocyte density significantly increased (19%; $p < 0.02$) while the TIEG1 KO osteocyte density significantly decreased (17%; $p < 0.01$). Between three and eight months of age, the WT osteocyte density was significantly decreased (20%; $p < 0.005$) while the TIEG1 KO osteocyte density was unchanged [Fig. 5(b)].

DISCUSSION

The data presented in this manuscript reveal significant differences in the number and morphological properties of osteocytes located in the femurs of TIEG1 KO mice. These differences suggest an important role for TIEG1 in osteocyte development and density, as well as in the regulation of the hypomineralized perilacunar bone matrix.

Using transmission electron microscopy, we observed an area immediately surrounding osteocytes in WT bone that is visually represented by a light halo which corresponds to a lack of mineralization in this bone area. A similar observation was found by Lane *et al.*,[19] which analyzed the effect of glucocorticoids on trabecular bone matrix. The authors of this study also observed a sphere of hypomineralized matrix immediately surrounding osteocytes in glucocorticoid-treated animals. In the present study, this hypomineralized matrix was two-fold greater in WT mice than in TIEG1 KO mice for all of the age groups analyzed. Although the role of this hypomineralized surface is not yet understood, it seems that the TIEG1 transcription factor is necessary for its formation. These local changes in the bone matrix surrounding the osteocytes of TIEG1 KO mice may in part explain the previously described decrease in cortical bone strength, as well as the osteoporotic bone phenotype observed in these animals.[3] Some studies suggest that this hypomineralized area is reflective of the ability of osteocytes to remodel their local environment.[2] Thus, osteocyte metabolism and function may also be altered in the absence of TIEG1 expression leading to modifications of the hypomineralized surface. You *et al.*[37] described a fiber matrix surrounding osteocytes that may be involved in mechanosensing, allowing for amplification of external stimuli at the cellular level. Since there is very little of this hypomineralized bone matrix surrounding the osteocytes of TIEG1 KO mice, it is likely that there are significant defects in the mechanosensing ability of these cells which ultimately leads to defects in bone remodeling.

In addition to their role as mechanosensors, osteocytes also control bone homeostasis by secreting several molecules such as prostaglandin E2 and I2,[18] nitric oxides[17] and sclerostin.[30] Sclerostin is an inhibitor of bone formation and is reported to be a negative regulator of the bone forming activity of osteoblasts.[30,31,36] The absence of sclerostin protein is known to result in increased bone mass leading to the clinical disorder of sclerosteosis.[1,6] It is therefore likely that sclerostin acts as a regulatory signal governing bone microarchitecture and remodeling.[23,28,30] Based on the observed changes in the bone matrix surrounding TIEG1 KO osteocytes, it is possible that the loss of TIEG1 expression in these cells alters the expression of specific genes necessary for normal bone maintenance.

We have also identified a significant decrease in osteocyte area in the femurs of TIEG1 KO mice at three months of age relative to WT controls. Interestingly, no changes were observed at the one- and eight-month time points. These data suggest an age-dependent regulation of osteocyte development by TIEG1. These age-dependent changes correlate well with our previous studies demonstrating changes in tail tendon microarchitecture between WT and TIEG1 KO mice at three months of age, with no changes observed at one and fifteen months of age.[4] Furthermore, a greater difference (59%) in the hypomineralized surface (*HS*) was found at three months of age between WT and TIEG1 KO osteocytes compared to the one-month (56%) and eight-month (41%) time points.

Through the analysis of osteocyte density in femurs isolated from WT and TIEG1 KO mice, we demonstrate that osteocyte number is significantly reduced in the TIEG1 KO animals at each of the age groups tested. This result is in agreement with our previous report which demonstrated that, at three months of age, TIEG1 KO mice display decreased osteocyte density relative to WT controls.[3] These data also correlate with the study of Subramaniam *et*

al. which demonstrated that TIEG1 KO osteoblasts are unable to fully differentiate and mineralize in culture,[27] raising the hypothesis that the lack of osteocytes in KO mouse femurs may be due to defects in the final stages of osteoblast maturation and/or differentiation.

We have previously shown that adult TIEG1 KO mice displayed a significant bone phenotype described as osteoporotic.[3] TIEG1 is known to be highly expressed in bones compared to other tissues,[26] and is involved in regulating the expression of other important osteoblast marker genes including alkaline phosphatase, Runx2, osterix and osteocalcin. In addition to osteoblast cells, the present study has demonstrated the impact of TIEG1 on osteocyte cells. Indeed, the decrease of hypomineralized perilacunar matrix in TIEG1 KO mice may be due to a defect in the metabolism of osteocytes, which may alter the ability of these cells to remodel their hypomineralized surrounding bone matrix. Metabolism changes found in osteocyte cells may in part explain the osteoporotic bone phenotype characterizing TIEG1 KO mice.

In summary, our data indicate that the lack of TIEG1 expression results in a significant decrease in osteocyte surface, osteocyte density and the surrounding hypomineralized bone matrix. While little is known about the function or importance of this hypomineralized bone matrix immediately adjacent to osteocytes, this study reveals significant differences in this bone microenvironment and suggests that osteocyte function may be compromised in the absence of TIEG1 expression.

Acknowledgments

We would like to thank Trace Christensen for his helpful discussions and comments as well as for his assistance with the transmission electron microscopy acquisition. This work was in part supported by an NIH grant DE14036 (TCS).

References

1. Balemans W, Ebeling M, Patel N, Van Hul E, Olson P, Dioszegi M, Lacza C, Wuyts W, et al. Increased bone density in sclerosteosis is due to the deficiency of a novel secreted protein (SOST). Hum Mole Genet. 2001; 10:537–543.
2. Baylink DJ, Wergedal JE. Bone formation by osteocytes. Am J Physiol. 1971; 221:669–678. [PubMed: 5570322]
3. Bensamoun SF, Hawse JR, Subramaniam M, Ilharreborde B, Bassillais A, Benhamou CL, Fraser DG, Oursler MJ, Amadio PC, An KN, Spelsberg TC. TGF*β* inducible early gene-1 knockout mice display defects in bone strength and microarchitecture. Bone. 2006; 39:1244–1251. [PubMed: 16876494]
4. Bensamoun SF, Tsubone T, Subramaniam M, Hawse JR, Boumediene E, Spelsberg TC, An KN, Amadio PC. Age-dependent changes in the mechanical properties of tail tendons in TGF-beta inducible early gene-1 knockout mice. J Appl Physio. 2006; 101(5):1419–1424.
5. Bonewald LF. Mechanosensation and transduction in osteocytes. Bonekey Osteovision. 2006; 3:7–15. [PubMed: 17415409]
6. Brunkow ME, Gardner JC, Van Ness J, Paeper BW, Kovacevich BR, Proll S, Skonier JE, et al. Bone dysplasia sclerosteosis results from loss of the SOST gene product, a novel cystine knot-containing protein. Am J Hum Genet. 2001; 68:577–589. [PubMed: 11179006]
7. Cowin SC, Weinbaum S, Zeng Y. A case for bone canaliculi as the anatomic site of strain generated potentials. J Biomech. 1995; 28:1281–1297. [PubMed: 8522542]
8. Duncan RL, Misler S. Voltage-activated and stretch-activated Ba21 conducting channels in an osteoblast-like cell line (UMR-106). Fed Eur Bone Soc Lett. 1989; 251:17–21.
9. Feng JQ, Ward LM, Liu S, Lu Y, Xie Y, Yuan B, Yu X, Rauch F, Davis SI, Zhang S, Rios H, Drezner MK, Quarles LD, Bonewald LF, White KE. Loss of DMP1 causes rickets and osteomalacia

and identifies a role for osteocytes in mineral metabolism. Nat Genet. 2006; 38:1310–1315. [PubMed: 17033621]

10. Filvaroff E, Erlebacher A, Ye J, Gitelman SE, Lotz J, Heillman M, Derynck R. Inhibition of TGF-beta receptor signaling in osteoblasts leads to decreased bone remodeling and increased trabecular bone mass. Development. 1999; 126:4267–4279. [PubMed: 10477295]
11. Geiser AG, Zeng QQ, Sato M, Helvering LM, Hirano T, Turner CH. Decreased bone mass and bone elasticity in mice lacking the transforming growth factor-beta1 gene. Bone. 1998; 23:87–93. [PubMed: 9701466]
12. Harrigan TP, Hamilton JJ. Bone strain sensation via transmembrane potential changes in surface osteoblasts: Loading rate and microstructural implications. J Biomech. 1993; 26:183–200. [PubMed: 8429060]
13. Hawse JR, Iwaniec UT, Bensamoun SF, Monroe DG, Peters KD, Ilharreborde B, Rajamannan NM, Oursler MJ, Turner RT, Spelsberg TC, Subramaniam M. TIEG-null mice display an osteopenic gender-specific phenotype. Bone. 2008; 42:1025–1031. [PubMed: 18396127]
14. Irie K, Ejiri S, Sakakura Y, Shibui T, Yajima T. Matrix mineralization as a trigger for osteocyte maturation. J Histochem Cytochem. 2008; 56:561–567. [PubMed: 18319272]
15. Johnsen SA, Subramaniam M, Janknecht R, Spelsberg TC. TGFbeta inducible early gene enhances TGFbeta/Smad-dependent transcriptional responses. Oncogene. 2002; 21:5783–5790. [PubMed: 12173049]
16. Joyce ME, Roberts AB, Sporn MB, Bolander ME. Transforming growth factor-beta and the initiation of chondro-genesis and osteogenesis in the rat femur. J Cell Biol. 1990; 110:2195–2207. [PubMed: 2351696]
17. Klein-Nulend J, Semeins CM, Ajubi NE, Nijweide PJ, Burger EH. Pulsating fluid flow increases nitric oxyde (NO) synthesis by osteocytes but not periosteal fibroblasts- correlation with prostaglandin upregulation. Biochem Biophys Res Commun. 1995; 217:640–648. [PubMed: 7503746]
18. Klein-Nulend J, van der Plas A, Semeins CM, Ajubi NE, Frangos JA, Nijweide PJ, Burger EH. Sensitivity of osteocytes to biomechanical stress *in vitro*. FASEB J. 1995; 9:441–445. [PubMed: 7896017]
19. Lane NE, Yao W, Balooch M, Nalla RK, Balooch G, Habelitz S, Kinney JH, Bonewald LF. Glucocorticoid-treated mice have localized changes in trabecular bone material properties and osteocyte lacunar size that are not observed in placebo-treated or estrogen-deficient mice. J Bone Miner Res. 2006; 1:466–476. [PubMed: 16491295]
20. Martin RB. Toward a unifying theory of bone remodeling. Bone. 2000; 26:1–6. [PubMed: 10617150]
21. Marotti G. The osteocyte as a wiring transmission system. J Musculoskel Neuron Interact. 2000; 1:133–136.
22. McCreadie BR, Hollister SJ, Schaffler MB, Goldstein SA. Osteocyte lacuna size and shape in women with and without osteoporotic fracture. J Biomech. 2004; 37:563–572. [PubMed: 14996569]
23. Poole KES, van Bezooijen RL, Loveridge N, Hamersma H, Papapoulos SE, Löwik CW, Reeve J. Sclerostin is a delayed secreted product of osteocytes that inhibits bone formation. FASEB J. 2005; 19:1842–1844. [PubMed: 16123173]
24. Rubin MA, Jasiuk I. The TEM characterization of the lamellar structure of osteoporotic human trabecular bone. Micron. 2005; 36:653–664. [PubMed: 16198582]
25. Subramaniam M, Harris SA, Oursler MJ, Rasmussen K, Riggs BL, Spelsberg TC. Identification of a novel TGF-beta-regulated gene encoding a putative zinc finger protein in human osteoblasts. Nucleic Acids Res. 1995; 23:4907–4912. [PubMed: 8532536]
26. Subramaniam M, Hefferan TE, Tau K, Peus D, Pittelkow M, Jalal S, Riggs BL, Roche P, Spelsberg TC. Tissue, cell type, and breast cancer stage-specific expression of a TGF-beta inducible early transcription factor gene. J Cell Biochem. 1998; 68:226–236. [PubMed: 9443078]
27. Subramaniam M, Gorny G, Johnsen SA, Monroe DG, Evans GL, Fraser DG, Rickard DJ, et al. TIEG1 null mouse-derived osteoblasts are defective in mineralization and in support of osteoclast differentiation *in vitro*. Mol Cell Biol. 2005; 25:1191–1199. [PubMed: 15657444]

28. Sutherland MK, Geoghegan JC, Yu C, Turcott E, Skonier JE, Winkler DG, Latham JA. Sclerostin promotes the apoptosis of human osteoblastic cells: A novel regulation of bone formation. Bone. 2004; 35:828–835. [PubMed: 15454089]
29. Tachibana I, Imoto M, Adjei PN, Gores GJ, Subramaniam M, Spelsberg TC, Urrutia R. Overexpression of the TGFbeta-regulated zinc finger encoding gene, TIEG, induces apoptosis in pancreatic epithelial cells. J Clin Invest. 1997; 99:2365–2374. [PubMed: 9153278]
30. van Bezooijen RL, Roelen BA, Visser A, van der Wee-Pals L, de Wilt E, Karperien M, Hamersma H, Papapoulos SE, ten Dijke P, Lowik CW. Sclerostin is an osteocyte-expressed negative regulator of bone formation, but not a classical BMP antagonist. J Exp Med. 2004; 199:805–814. [PubMed: 15024046]
31. van Bezooijen RL, Svensson JP, Eefting D, Visser A, van der Horst G, Karperien M, et al. Wnt but not BMP signaling is involved in the inhibitory action of sclerostin on BMP-stimulated bone formation. J Bone Mineral Res. 2007; 22:19–28.
32. Vashishth D, Verborgt O, Divine G, Schaffler MB, Fyhrie DP. Decline in osteocyte lacunar density in human cortical bone is associated with accumulation of microcracks with age. Bone. 2000; 26:375–380. [PubMed: 10719281]
33. Vatsa A, Breuls RG, Semeins CM, Salmon PL, Smit TH, Klein-Nulend J. Osteocyte morphology in fibula and calvaria – is there a role for mechanosensing? Bone. 2008; 43:452–458. [PubMed: 18625577]
34. Wang Z, Peters B, Klussmann S, Bender H, Herb A, Krieglstein K. Gene structure and evolution of Tieg3, a new member of the Tieg family of proteins. Gene. 2004; 325:25–34. [PubMed: 14697507]
35. Weinbaum S, Cowin SC, Zeng Y. A model for the excitation of osteocytes by mechanical loading-induced bone fluid shear stresses. J Biomech. 1994; 27:339–360. [PubMed: 8051194]
36. Winkler DG, Sutherland MK, Geoghegan JC, Yu C, Hayes T, Skonier JE, Shpektor D, et al. Osteocyte control of bone formation via sclerostin, a novel BMP antagonist. EMBO J. 2003; 22:6267–6276. [PubMed: 14633986]
37. You LD, Weinbaum S, Cowin SC, Schaffler MB. Ultra-structure of the osteocyte process and its pericellular matrix. Anat Rec. 2004; 278A:505–513.

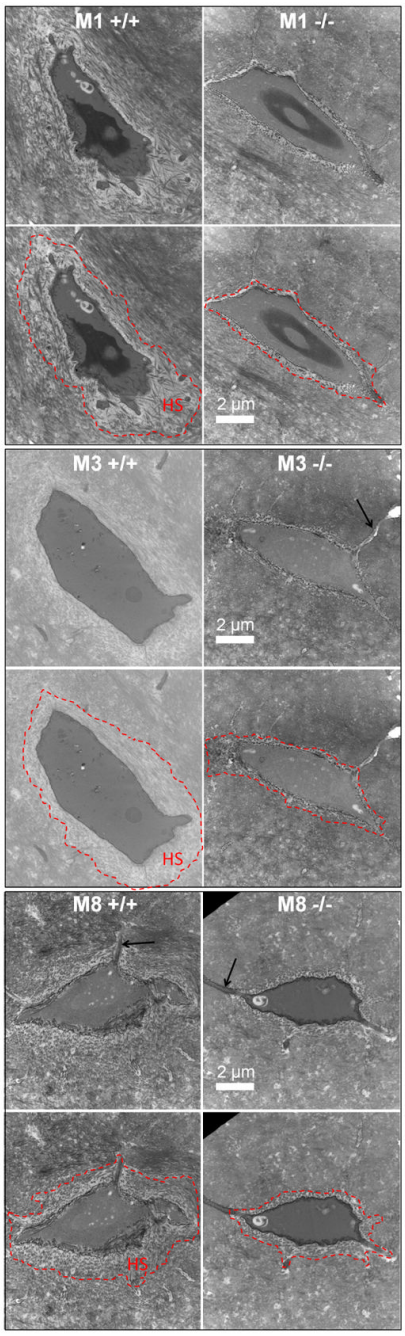

Fig. 1.

TEM micrograph (×11, 000) of osteocytes located in the endosteal portion of the femur from one-month (M1), three-month (M3) and 8-month (M8) old WT (+/+) and TIEG1 KO (−/−) mice. The hypomineralized surface (*HS*) is located between the border of the cell and the dotted line. Black arrow indicates canaliculi. Bar = 2 μm.

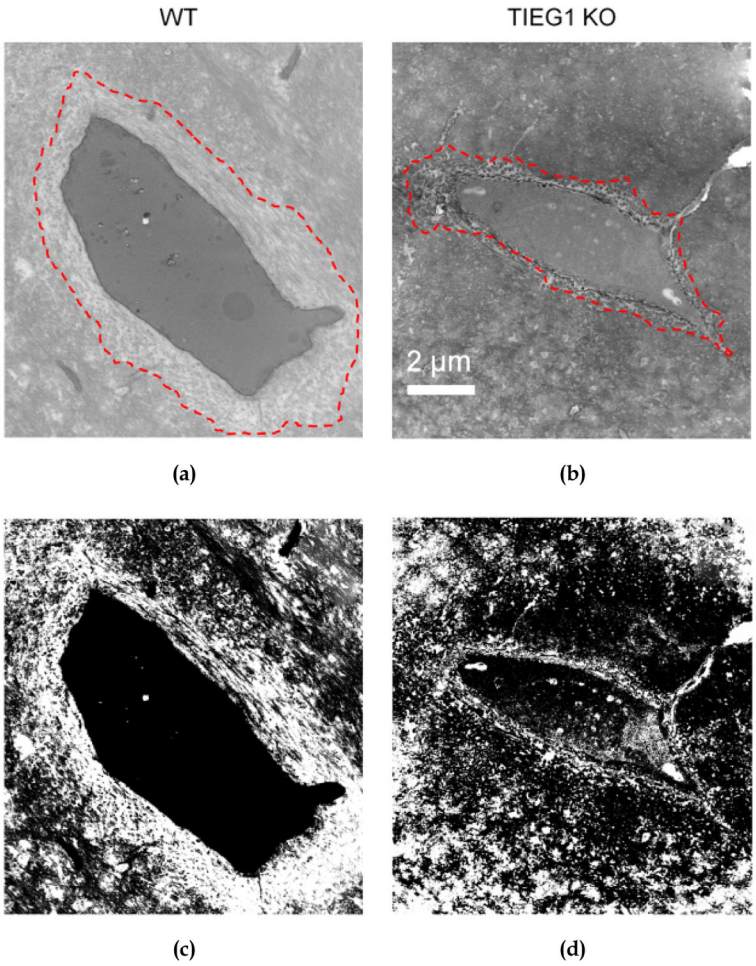

Fig. 2.

(a) and **(b)**: TEM micrograph (×11, 000) of endosteal osteocytes from three-month-old WT **(a)** and TIEG1 KO **(b)** mice femur. The hypomineralized surface is located between the border of the cell and the dotted red line. Bar 2 μm. **(c)** and **(d)**: Binary images after thresholding of the WT **(c)** and TIEG1 KO **(d)** TEM images, allowing for determination of the border of the hypomineralized surface.

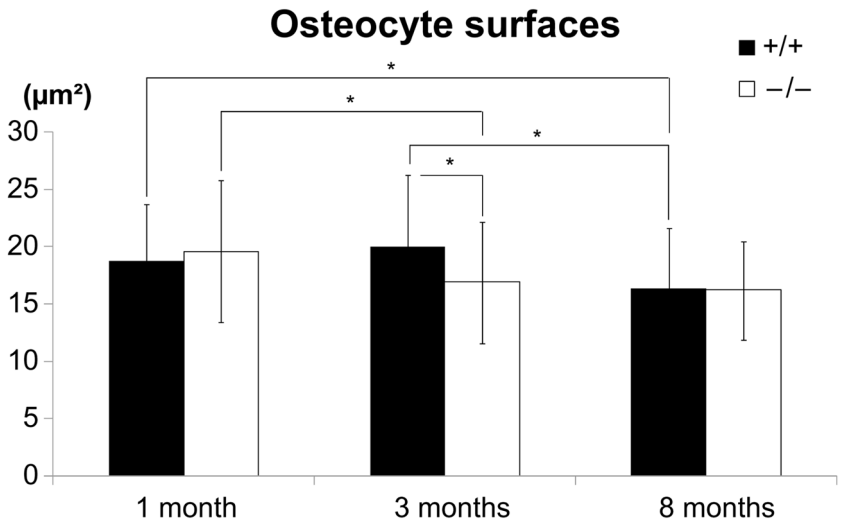

Fig. 3.

Osteocyte surface for WT (+/+) and TIEG1 KO (−/−) mice as a function of age. The diagram shows mean surfaces ± SD. (* $p < 0.05$)

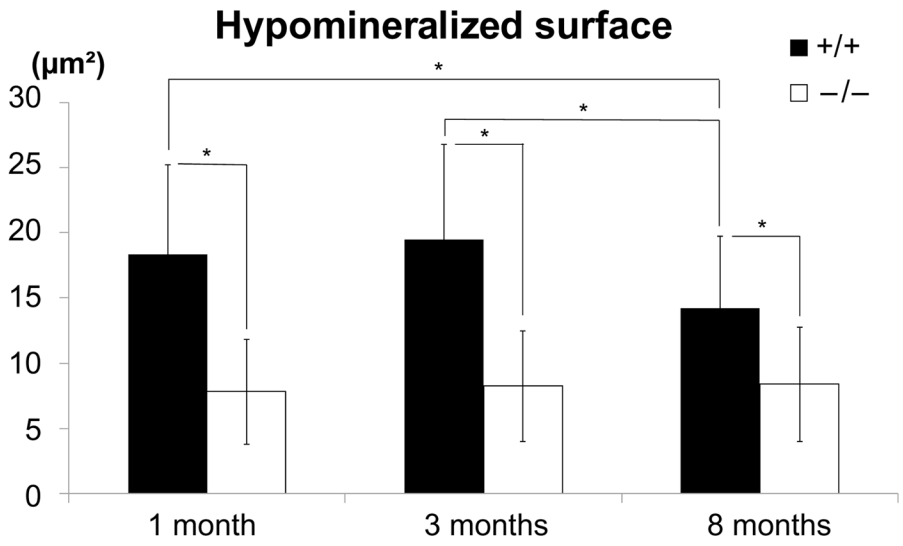

Fig. 4.

Area of hypomineralized surface surrounding femoral osteocytes in WT (+/+) and TIEG1 KO (−/−) mice as a function of age. The diagram shows mean surfaces ± SD. (* $\boldsymbol{p} < 0.01$)

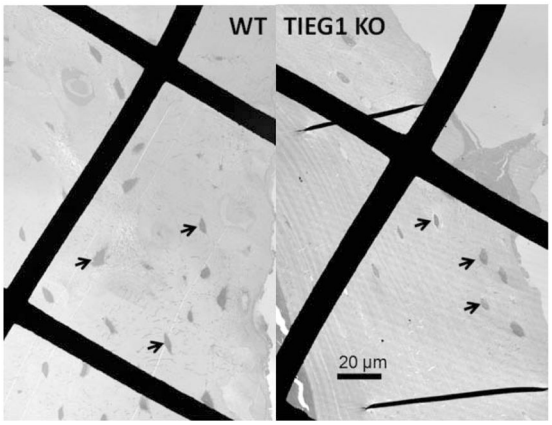

(a)

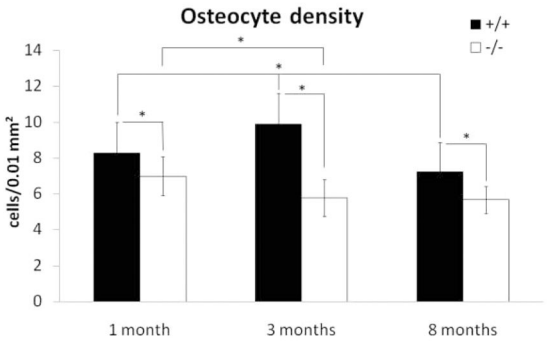

(b)

Fig. 5.

(a) Representative transmission electron microscopy images (×1000) depicting osteocytes (black arrows) in the femoral cortical region of three-month-old WT and TIEG1 KO mice. **(b)** Changes in osteocyte density for WT (+/+) and TIEG1 KO (−/−) mice as a function of age. The diagram shows the average number of osteocytes (per 100 μm^2) ± SD. (* $p < 0.01$)